Modeling Power Saving for GAN and UMTS Interworking

Shun-Ren Yang[*], Phone Lin[†], and Pei-Tang Huang[‡]

Abstract

3GPP 43.318 specifies the *Generic Access Network* (GAN) for interworking between *Wireless Local Area Network* (WLAN) and *Universal Mobile Telecommunications System* (UMTS) core network. A dual-mode *Mobile Station* (MS) is equipped with two communication modules to support both WLAN and UMTS radio technologies, which shortens the battery lifetime of the MS. This paper proposes an analytical model and conducts simulation experiments to study the power consumption of dual-mode MSs in terms of the *power consumption indicator* and *mean packet waiting time*. Our study provides guidelines for designing WLAN-UMTS dual-mode MSs.

Keywords: Generic Access Network (GAN), Power Saving, Universal Mobile Telecommunications System (UMTS), Wireless Local Area Network (WLAN).

1 Introduction

IEEE 802.11 *Wireless Local Area Network* (WLAN) provides users high bit-rate wireless transmission service within hot-spot areas, e.g., indoor or basement. On the other hand,

[*]Shun-Ren Yang is with Department of Computer Science and Institute of Communications Engineering, National Tsing Hua University, Hsinchu, Taiwan, R.O.C. Yang's e-mail address is sryang@cs.nthu.edu.tw.

[†]Corresponding Author: Phone Lin is with Department of Computer Science and Information Engineering, Graduate Institute of Networking and Multimedia, National Taiwan University, Taipei, Taiwan, R.O.C. Lin's e-mail address is plin@csie.ntu.edu.tw.

[‡]Pei-Tang Huang is with Department of Computer Science and Information Engineering, National Taiwan University, Taipei, Taiwan, R.O.C. Huang's email address is tang@pcs.csie.ntu.edu.tw.

3GPP *Universal Mobile Telecommunications System* (UMTS) provides wireless transmission service within wide areas and supports high user mobility. WLAN and UMTS are treated as complementary wireless network technologies [6]. To provide users wireless access service to networks irrespective of their locations and network access technologies, the *Unlicensed Mobile Access* (UMA) technology [18] is proposed for interworking and integration between UMTS and WLAN, which has been proven and accommodated in 3GPP 43.318 [1]. The *Generic Access Network* (GAN) is defined in 3GPP 43.318 to enable WLAN to connect to the UMTS core network.

GAN provides UMTS subscribers with the low-cost and high-speed WLAN access. However, a dual-mode *Mobile Station* (MS) is equipped with two communication modules for both WLAN and UMTS radio technologies. The work in [17] showed that the battery lifetime will be significantly shortened while an additional WLAN module is added to an MS. Therefore, how to reduce dual-mode MS power consumption is an important issue, which may reflect the user satisfaction with the offered wireless access service. Many research efforts in the literature have dedicated to the investigation of the MS power saving mechanisms in different wireless mobile networks, e.g., [14] for CDPD, [19] for UMTS, [12] for both UMTS and cdma2000, and [20] for IEEE 802.11 WLAN. Nevertheless, all of these studies only considered the power consumption behavior of single-mode MSs. To the best of our knowledge, there is no previous work covering the "power saving of a dual-mode MS" topic.

This paper proposes an analytical model to study the power consumption issue for MSs operating in the GAN and UMTS interworking network. The model quantifies the power consumption of a WLAN-UMTS dual-mode MS, which is referred to as the *power consumption indicator*. It is clear that the lower the power consumption indicator, the more effective the utilized power management technique. However, reducing the power consumption may at the same time degrade the system performance in terms of service delay. Therefore, we also quantify the *mean packet waiting time* to examine the penalty caused by exercising the power saving mechanism for GAN-UMTS interworking. Due to the complicated behavior of a dual-mode MS, the proposed analytical model may not well capture the MS behavior under some conditions. To release these constraints of the analytical model, we conduct simulation experiments as well. We note that the performance of a power saving mechanism primarily depends on MSs' uplink and downlink packet transmission/reception behavior.

Whenever an MS has uplink packets to transmit, it can immediately terminate the power saving operation and switch into the power active state for packet delivery. On the other hand, for the downlink packet reception, it is very difficult for MSs to predict the instants of the subsequent packet arrivals. In this case, an MS can not adjust its power management state proactively to adapt to the downlink packet traffic. This paper will concentrate on the more challenging power management for MS downlink packet transmissions. The uplink performance metrics such as the transmission power consumption of MSs are therefore not discussed in this paper. Our work derives close-form equations for both the power consumption indicator and mean packet waiting time with the premise that the WLAN available and unavailable periods are sufficiently small. Furthermore, our study indicates that with proper parameter settings, power management techniques can reduce the power consumption indicator of a WLAN-UMTS dual-mode MS without significantly increasing the mean packet waiting time. The analytical and simulation results of this work can serve as guidelines for the implementation of WLAN-UMTS dual-mode MSs.

2 System Model

This section first gives an overview of the GAN-UMTS interworking architecture, and then describes the system model for our study of GAN-UMTS dual-mode MS power saving.

Figure 1 illustrates a simplified system architecture for the GAN-UMTS interworking, where GAN (Figure 1 (a)) is an alternative radio access network for the UMTS core network (Figure 1 (d)). We may apply any kind of IP access technologies in GAN, such as IEEE 802.11 [9] or Bluetooth [3]. This paper assumes IEEE 802.11 WLAN (Figure 1 (h)) as the underlying IP access technology in GAN. Both GAN and *UMTS Terrestrial Radio Access Network* (UTRAN; Figure 1 (b)) connect to *Serving GPRS Support Node* (SGSN; Figure 1 (c)) in the UMTS core network and receive packets destined to a dual-mode MS (Figure 1 (e)) from external IP networks (Figure 1 (j)). Functioning like *Radio Network Controller* (RNC; Figure 1 (f)) in UTRAN, *Generic Access Network Controller* (GANC; Figure 1 (g)) in GAN receives packets from SGSN and forwards them to the MS through *Access Points* (APs; Figure 1 (k)) in WLAN. While the MS leaves WLAN coverage, the SGSN may also forward the incoming packets to the RNC in the UTRAN. The RNC processor sends the packets to

the Node B (Figure 1 (l)) through an *Asynchronous Transfer Mode* (ATM; Figure 1 (m)) link. The Node B then delivers the packets to the MS through the *Wideband Code Division Multiple Access* (WCDMA) radio link.

To conserve the power budget of a GAN-UMTS dual-mode MS, the UMTS *Discontinuous Reception* (DRX) [2] and the IEEE 802.11 *Power Saving Mode* (PSM) [9] are employed, respectively. The concept of DRX is for an idle MS to power off the radio receiver for a predefined period (referred as *DRX cycle*) instead of continuously listening to the radio channel signal. As shown in Figure 2, the activities of an MS's UMTS receiver module under DRX can be characterized in terms of three periods:

Busy periods. During packet transmission to the MS, incoming packets are first stored in the RNC buffer before they are delivered to the MS. Then, the RNC processor transmits the packets in the *First In First Out* (FIFO) order.

Inactivity periods. When the RNC buffer becomes empty, the RNC inactivity timer is activated. If any packet arrives at the RNC before the inactivity timer expires, the timer is stopped. The RNC processor starts to transmit packets, and another busy period begins.

Sleep periods. If no packet arrives before the inactivity timer expires, the MS enters a sleep period, and the UMTS receiver module is turned off. The sleep period contains one or more DRX cycles. At the end of a DRX cycle, the MS wakes up to listen to the paging channel. If some packets have arrived at the RNC during the last DRX cycle, the MS starts to receive packets and the sleep period ends. Otherwise, the MS returns to sleep until the end of the next DRX cycle.

Note that during busy and inactivity periods, the MS turns on the UMTS receiver module.

Zheng *et al.* [20] have shown that the IEEE 802.11 PSM mechanism is oblivious of the packet traffic characteristics, and thus is not energy-efficient under light traffic load and suffer from significant performance degradation at higher traffic load in terms of power consumption and packet mean waiting time. Therefore, our system model considers UMTS DRX mechanism during packet transmission through UMTS but ignores IEEE 802.11 PSM during packet transmission through IEEE 802.11 WLAN.

As shown in Figure 3, since the WLAN can support higher data transmission rate and is of lower cost, we suppose that the SGSN delivers the packets to the GANC whenever possible. The SGSN could also utilize the global always-on UMTS connectivity for packet delivery when the MS leaves the WLAN hotspot coverage and the WLAN connection is not available. Suppose that packet arrivals for an MS to the SGSN form a Poisson stream with rate λ_a. We assume that the WLAN availability for the MS follows the ON-OFF patterns repeatedly. Specifically, the WLAN connectivity is available during an ON period, and is unavailable when the ON period ends. Then, the WLAN connectivity enters an OFF period. The ON and OFF periods are assumed to be exponentially distributed with rates λ_o and λ_f, respectively.

Due to the high wireless transmission rate feature of WLAN, we assume that each packet arrival to the GANC can be transmitted immediately, and no packet has to be buffered in the GANC. When packets arrive during a WLAN OFF period, they are forwarded to the RNC. In UTRAN, ATM is much faster and more reliable than the WCDMA wireless transmission. Therefore, we ignore the ATM transmission delay between the RNC and the Node B, and the RNC and the Node B are modeled as a FIFO queueing server. Let t_x denote the packet service time, i.e., the interval between the time when a packet is transmitted by the RNC processor and the time when the corresponding ack is received by the RNC processor. Let t_I be the threshold of the RNC inactivity timer, and t_D be the length of the UMTS DRX cycle. At the end of every DRX cycle, the MS must wake up for a short period τ so that it can listen to the paging information from the network. Therefore the "power saving" period in a DRX cycle is $t_D - \tau$.

3 An Analytic Model

This section proposes an analytical model to investigate the power consumption of a dual-mode MS. In the following, we first determine the packet arrival process to the RNC. Then, based on the inter-packet arrival time distribution to the RNC, we derive the following two output measures:

- the power consumption indicator P_i: the average power consumption of an MS's radio receivers (including the UMTS and the WLAN receiver modules) when the UMTS

DRX mechanism is exercised;

- the mean packet waiting time $E[t_w]$: the expected waiting time for a packet between the time when it is received by the SGSN and the time when it is transmitted by the GANC or the RNC to the MS.

As shown in Figure 3, two cases are considered to derive the probability density function $f_r(t)$ for the inter-packet arrival time t_r between two consecutive packet arrivals to the RNC.

Case 1. In this case, two consecutive packets, Packets 1 and 2, arrive at the SGSN within the same WLAN OFF period denoted as $t_{\mathrm{OFF},1}$, and both Packets 1 and 2 are forwarded to the RNC. Let t_1 and t_2 be the arrival time points of Packets 1 and 2, respectively. The interval $t_2 - t_1$ has the following probability density function

$$f_{t_2-t_1}(t) = f_a(t) \Pr[t_{\mathrm{OFF},1} > t], \tag{1}$$

where $f_a(t)$ is the probability density function of the inter-packet arrival time t_a to the SGSN, and $\Pr[t_{\mathrm{OFF},1} > t]$ is the probability that two consecutive packets arrive during $t_{\mathrm{OFF},1}$. Since t_a and $t_{\mathrm{OFF},1}$ are assumed to be exponentially distributed with rate λ_a and λ_f, (1) can be rewritten as

$$f_{t_2-t_1}(t) = e^{-\lambda_f t} \lambda_a e^{-\lambda_a t}. \tag{2}$$

In this case, the inter-packet arrival time t_r to the RNC equals to $t_2 - t_1$. Thus, the probability density function $f_r(t)$ for t_r is

$$f_r(t) = f_{t_2-t_1}(t) = e^{-\lambda_f t} \lambda_a e^{-\lambda_a t}. \tag{3}$$

Case 2. After the arrival of Packet 2, let Packet 3 arrival at t_3 be the first packet arrival during a WLAN OFF period. In this case, Packets 2 and 3 are separated by several packet arrivals within WLAN ON periods. The inter-packet arrival time t_r for Case 2 is equal to $t_3 - t_2$. Let t_f be the total length of WLAN OFF periods during $[t_2, t_3]$. Assume that there are n WLAN OFF periods $t_{\mathrm{OFF},1}$, $t_{\mathrm{OFF},2}$, ..., $t_{\mathrm{OFF},n}$ between t_2 and t_3. Denote $t'_{\mathrm{OFF},1}$ as the residual OFF period of $t_{\mathrm{OFF},1}$ at t_2 and $t'_{\mathrm{OFF},n}$ as the age OFF period of $t_{\mathrm{OFF},n}$ at t_3. Then,

$$t_f = t'_{\mathrm{OFF},1} + \left(\sum_{i=2}^{n-1} t_{\mathrm{OFF},i} \right) + t'_{\mathrm{OFF},n}. \tag{4}$$

As shown in Figure 3, no packet arrives during $t'_{\mathrm{OFF},1}$ (with probability $e^{-\lambda_a t'_{\mathrm{OFF},1}}$), $t_{\mathrm{OFF},2}$ (with probability $e^{-\lambda_a t_{\mathrm{OFF},2}}$), ..., and $t_{\mathrm{OFF},n-1}$ (with probability $e^{-\lambda_a t_{\mathrm{OFF},n-1}}$), and Packet 3 arrives at time $t'_{\mathrm{OFF},n}$ of the WLAN OFF period $t_{\mathrm{OFF},n}$ (with probability density function $\lambda_a e^{-\lambda_a t'_{\mathrm{OFF},n}}$). Therefore, the probability density function $f_f(t_f)$ for t_f is expressed as

$$\begin{aligned} f_f(t_f) &= e^{-\lambda_a t'_{\mathrm{OFF},1}} e^{-\lambda_a t_{\mathrm{OFF},2}} \cdots e^{-\lambda_a t_{\mathrm{OFF},n-1}} \lambda_a e^{-\lambda_a t'_{\mathrm{OFF},n}} \\ &= \lambda_a e^{-\lambda_a (t'_{\mathrm{OFF},1} + t_{\mathrm{OFF},2} + \cdots + t_{\mathrm{OFF},n-1} + t'_{\mathrm{OFF},n})} = \lambda_a e^{-\lambda_a t_f}. \end{aligned} \tag{5}$$

Let N_o be the number of WLAN ON periods during $[t_2, t_3]$, and t_o be the total length of these N_o WLAN ON periods. We proceed to derive the conditional probability mass function $\theta_{n|t_f} = \Pr[N_o = n|t_f]$ for N_o and the conditional probability density function $f_{o|t_f,N_o}(t_o|t_f, N_o = n)$ for t_o. In Figure 3, $t'_{\mathrm{OFF},1}$, $t_{\mathrm{OFF},i}$ $(2 \le i \le n-1)$, and $t'_{\mathrm{OFF},n}$ are all exponential random variables with rate λ_f. Therefore, it is clear that the number of WLAN ON periods has the Poisson distribution with rate λ_f, and we have

$$\theta_{n|t_f} = \Pr[N_o = n|t_f] = e^{-\lambda_f t_f} \frac{(\lambda_f t_f)^n}{n!}. \tag{6}$$

Conditioning on t_f (with probability $f_f(t_f)dt_f$) and $N_o = n$ (with probability $\theta_{n|t_f}$), the total length t_o of WLAN ON periods during $[t_2, t_3]$ is an Erlang-n random variable with rate λ_o and probability density function

$$f_{o|t_f,N_o}(t_o|t_f, N_o = n) = \frac{\lambda_o^n}{(n-1)!} t_o^{n-1} e^{-\lambda_o t_o}. \tag{7}$$

The $f_r(t)$ for the inter-packet arrival time t_r in this case can then be expressed in terms of $f_f(t_f)$, $\theta_{n|t_f}$ and $f_{o|t_f,N_o}(t_o|t_f, N_o = n)$ as

$$f_r(t) = \int_{t_f=0}^{t} f_f(t_f) \sum_{n=1}^{\infty} \theta_{n|t_f} f_{o|t_f,N_o}(t - t_f|t_f, N_o = n) dt_f. \tag{8}$$

Substitute (5), (6), and (7) into (8) to obtain

$$f_r(t) = \int_{t_f=0}^{t} \lambda_a e^{-\lambda_a t_f} \sum_{n=1}^{\infty} e^{-\lambda_f t_f} \left[\frac{(\lambda_f t_f)^n}{n!}\right] \left[\frac{\lambda_o^n}{(n-1)!}\right] (t - t_f)^{n-1} e^{-\lambda_o (t - t_f)} dt_f. \tag{9}$$

Combining (3) and (9), we derive the probability density function $f_r(t)$ for the inter-packet arrival time t_r to the RNC

$$f_r(t) = e^{-\lambda_f t} \lambda_a e^{-\lambda_a t} + \int_{t_f=0}^{t} \lambda_a e^{-\lambda_a t_f} \sum_{n=1}^{\infty} e^{-\lambda_f t_f} \left[\frac{(\lambda_f t_f)^n}{n!}\right] \left[\frac{\lambda_o^n}{(n-1)!}\right] (t - t_f)^{n-1} e^{-\lambda_o (t - t_f)} dt_f. \tag{10}$$

Equation (10) is too complicated for the analysis of P_i and $E[t_w]$. With the following theorem, we attempt to obtain a simpler $f_r(t)$ probability density function.

Theorem 1 *When $\lambda_o \to \infty$, $\lambda_f \to \infty$ and $\frac{\lambda_f}{\lambda_o} \to C > 0$ where C is a constant, we have that the inter-packet arrival time t_r to the RNC follows an exponential distribution with rate $\frac{\lambda_a}{1+C}$.*

Proof. Since $N_o|t_f$ is a Poisson random variable with rate λ_f (see (6)), we have

$$E[N_o|t_f] = \lambda_f t_f \text{ and } Var[N_o|t_f] = \lambda_f t_f. \tag{11}$$

Furthermore, $t_o|t_f, N_o = n$ is an Erlang-n random variable with rate λ_o (see (7)), and therefore

$$E[t_o|t_f, N_o = n] = \frac{n}{\lambda_o} \text{ and } Var[t_o|t_f, N_o = n] = \frac{n}{\lambda_o^2}. \tag{12}$$

Using expectation by conditioning technique [16], we have that

$$E[t_o|t_f] = E[E[t_o|t_f, N_o]|t_f]. \tag{13}$$

From (11) and (12), (13) is rewritten as

$$E[t_o|t_f] = E\left[\frac{N_o}{\lambda_o}\middle| t_f\right] = \frac{\lambda_f t_f}{\lambda_o}. \tag{14}$$

According to [16, page 51], the variance $Var[t_o|t_f]$ can be expressed as

$$Var[t_o|t_f] = Var[E[t_o|t_f, N_o]|t_f] + E[Var[t_o|t_f, N_o]|t_f]. \tag{15}$$

Substitute (11) and (12) into (15) to yield

$$Var[t_o|t_f] = Var\left[\frac{N_o}{\lambda_o}\middle| t_f\right] + E\left[\frac{N_o}{\lambda_o^2}\middle| t_f\right] = \frac{\lambda_f t_f}{\lambda_o^2} + \frac{\lambda_f t_f}{\lambda_o^2} = \frac{2\lambda_f t_f}{\lambda_o^2}. \tag{16}$$

From (14) and (16), it is clear that when $\lambda_o \to \infty$, $\lambda_f \to \infty$ and $\frac{\lambda_f}{\lambda_o} \to C$, $E[t_o|t_f] \to Ct_f$ and $Var[t_o|t_f] \to 0$, that is, $t_o|t_f$ converges to a constant Ct_f. In this case, we have

$$\begin{aligned} \Pr[t_r \le t] &= \Pr[t_o + t_f \le t] \\ &\to \Pr[t_f + Ct_f \le t] = \Pr\left[t_f \le \frac{t}{1+C}\right] = 1 - e^{-\left(\frac{\lambda_a}{1+C}\right)t}. \end{aligned}$$

Namely, t_r has the exponential distribution with rate $\frac{\lambda_a}{1+C}$. ■

Based on Theorem 1, we suppose that the inter-packet arrival time t_r to the RNC is exponentially distributed with rate $\lambda_r = \frac{\lambda_a}{1+C}$, and we can obtain close-form equations for P_i and $E[t_w]$.

The activities of an MS's UMTS receiver module can be characterized by a *regenerative process* [16], where a regeneration cycle consists of an inactivity period t_I^*, a sleep period t_S^* and a busy period t_B^* [19]. Let $P_{u,b}$, $P_{u,i}$, $P_{u,s}$, and $P_{u,l}$ be the power consumption (in watts) of the UMTS receiver module in the UMTS busy period, inactivity period, sleep period, and listening period (at the end of each DRX cycle), respectively. Let $P_{w,o}$ and $P_{w,f}$ be the power consumption (in watts) of the WLAN receiver module when the WLAN connection is available and unavailable, respectively. Suppose that there are N DRX cycles in a sleep period. Based on [16, Theorem 3.7.1], the average power consumption $P_{i,u}$ of the UMTS receiver module can be expressed as

$$P_{i,u} = \frac{E[t_I^*]P_{u,i} + (E[t_S^*] - E[N]\tau)P_{u,s} + E[N]\tau P_{u,l} + E[t_B^*]P_{u,b}}{E[t_I^*] + E[t_S^*] + E[t_B^*]}. \tag{17}$$

Suppose that the t_x distribution has mean $1/\lambda_x$ and variance V_x. Let $t_I = 1/\lambda_I$ and $t_D = 1/\lambda_D$. $E[t_I^*]$, $E[t_S^*]$, $E[N]$, and $E[t_B^*]$ have been derived in [19], which are expressed as

$$E[t_I^*] = \left(\frac{1}{\lambda_r}\right)\left(1 - e^{-\lambda_r/\lambda_I}\right),\ E[t_S^*] = \frac{e^{-\lambda_r/\lambda_I}}{(1 - e^{-\lambda_r/\lambda_D})\lambda_D},\ E[N] = \frac{e^{-\lambda_r/\lambda_I}}{1 - e^{-\lambda_r/\lambda_D}},$$
$$\text{and } E[t_B^*] = \frac{\rho[\lambda_D(1 - e^{-\lambda_r/\lambda_I})(1 - e^{-\lambda_r/\lambda_D}) + \lambda_r e^{-\lambda_r/\lambda_I}]}{\lambda_r\lambda_D(1 - e^{-\lambda_r/\lambda_D})(1 - \rho)}, \tag{18}$$

where $\rho = \lambda_r/\lambda_x$. Substituting (18) into (17), we could obtain $P_{i,u}$. Similarly, the activities of an MS's WLAN receiver module can be characterized by an *alternating ON-OFF process* [16]. Therefore, the average power consumption $P_{i,w}$ of the WLAN receiver module is

$$P_{i,w} = \frac{\lambda_f P_{w,o} + \lambda_o P_{w,f}}{\lambda_o + \lambda_f}. \tag{19}$$

Combine (17) and (19) to have the power consumption indicator $P_i = P_{i,u} + P_{i,w}$.

The UMTS DRX can be modeled as a variant of the $M/G/1$ queue with multiple vacations [19], and we have derived the mean packet waiting time $E[t_{w,u}]$ in the RNC buffer in [19]. The derivation of $E[t_{w,u}]$ is summarized as follows. By constructing an embedded Markov chain for the queue length of the RNC buffer, we can first obtain the probability generating function for the steady-state queue length distribution. Then, with this probability generating function and based on [5, Theorem 4.2], we can further derive the Laplace

transform for the packet waiting time $t_{w,u}$. (Let $\tilde{x}$ denote a random period of time, and let $F^*_{\tilde{x}}(s)$ denote the Laplace transform of $\tilde{x}$. Let $\tilde{y}$ denote the number of events from a Poisson process with rate λ that occur during the period of time $\tilde{x}$. [5, Theorem 4.2] states that the probability generating function $\mathcal{F}_{\tilde{y}}(z)$ for $\tilde{y}$ is given by $F^*_{\tilde{x}}(\lambda[1-z])$.) Finally, the mean packet waiting time $E[t_{w,u}]$ of $t_{w,u}$ can be obtained from its Laplace transform by using differentiation, and is expressed as

$$E[t_{w,u}] = \frac{\lambda_r e^{-\lambda_r/\lambda_I}}{2[\lambda_D^2(1-e^{-\lambda_r/\lambda_I})(1-e^{-\lambda_r/\lambda_D})+\lambda_r\lambda_D e^{-\lambda_r/\lambda_I}]} + \frac{\lambda_r(1+V_x\lambda_x^2)}{2(1-\rho)\lambda_x^2}. \quad (20)$$

Note that a packet will be served by the RNC only if it arrives at the SGSN during a WLAN OFF period (with probability $\frac{\lambda_o}{\lambda_o+\lambda_f}$). Therefore, the mean packet waiting time $E[t_w]$ is

$$E[t_w] = \left(\frac{\lambda_o}{\lambda_o+\lambda_f}\right) E[t_{w,u}]. \quad (21)$$

Substituting (20) into (21), we have the close-form equation for $E[t_w]$.

The analytical model are validated against the simulation experiments. The simulation model follows an event-driven approach which has been widely adopted in many mobile networking studies [11, 13]. The details of the simulation model are described in Appendix A. In the simulation model, we consider a more general case, i.e., release the assumptions in Theorem 1. Table 1 compares the analysis and simulation results for P_i and $E[t_w]$, where following Theorem 1, we set $V_x = 1/\lambda_x^2$, $t_I = 60/\lambda_x$, $t_D = 10/\lambda_x$, $\tau = 0.1/\lambda_x$, and $\lambda_a = 0.1\lambda_x$, and following the statistics data in [4], we set $P_{u,b} = 1.8$, $P_{u,i} = 0.4$, $P_{u,s} = 0.004$, $P_{u,l} = 0.5$, $P_{w,o} = 0.6$, and $P_{w,f} = 0.002$ (all in watts). The table indicates that the error rate (discrepancy) between analysis and simulation is within 0.41% in all cases. It is clear that the analysis is consistent with the simulation results. Table 1 also shows that $\lambda_o \geq 10^1\lambda_x$ is sufficient for ensuring the applicability of Theorem 1.

4 Performance Evaluation

This section investigates the P_i and $E[t_w]$ performance for a dual-mode MS based on our simulation experiments. We adopt the ETSI traffic model [7] as the packet traffic model destined to the MS. The ETSI model has been widely used to simulate the real packet traffic very well [8, 15].

Figure 4 illustrates the characteristic of a service session defined in the ETSI traffic model. Define the time interval between two consecutive service sessions as "the inter-session idle time", which is modeled as an exponential random variable with mean $1/\lambda_{is}$. A service session consists of one or more packet calls (Figure 4 (a)). The number of packet calls in a service session is modeled as a geometric random variable with mean μ_{pc}. In each packet call, there are one or more packets. The number of packets (Figure 4 (b)) in a packet call is modeled as a geometric random variable with mean μ_p. The inter-packet arrival time (Figure 4 (c)) within a packet call is modeled as an exponential random variable with mean $1/\lambda_p$. Define the time interval between two consecutive packet calls as "the reading time" (Figure 4 (d)), which is modeled as an exponential random variable with mean $1/\lambda_{pc}$. The packet size s_p (i.e., the number of bytes in a packet; Figure 4 (e)) is modeled as a Pareto random variable with cut-off. A normal Pareto distribution [10] (without cut-off) has two parameters β and l, where β describes the "heaviness" of the tail. The probability density function of a normal Pareto distribution is

$$f_P(x) = \left(\frac{\beta}{l}\right)\left(\frac{l}{x}\right)^{\beta+1} \text{ and the expected value is } E[P] = \left(\frac{\beta}{\beta-1}\right) l.$$

If β is between 1 and 2, then the variance for the distribution becomes infinity. A upper-bound m is used to set the maximum allowed size of a packet. Following the recommendation in [7], we model the packet size s_p as

$$\text{Packet Size } s_p = \min(P, m),$$

where P is a normal Pareto distributed random variable with $\beta = 1.1$, $l = 81.5$ bytes, and $m = 66666$ bytes. The mean packet size $E[s_p]$ is calculated in [7] as 480 bytes. The service time t_x (with mean $E[t_x] = 1/\lambda_x$) for a packet is derived from s_p, and is expressed as

$$t_x = \frac{8 \times \text{Packet Size } s_p}{\text{Transmission Bit Rate}}. \tag{22}$$

Figures 5-7 plot the P_i and $E[t_w]$ curves. Following the statistical data in [4], we set $P_{u,b} = 1.8$, $P_{u,i} = 0.4$, $P_{u,s} = 0.004$, $P_{u,l} = 0.5$, $P_{w,o} = 0.6$, and $P_{w,f} = 0.002$ (all in watts). Other parameter settings are described in the captions of the figures.

Effects of the ratio λ_f/λ_o. Figures 5-7 show the effects of λ_f/λ_o on P_i and $E[t_w]$. In the three figures, we observe that in most cases, P_i increases as λ_f/λ_o increases. The larger

λ_f/λ_o ratio results in the higher probability that the WLAN connection is available. Thus, less packets are served by the RNC. The WLAN receiver module is likely to be powered on, and the UMTS receiver module is likely to be switched to the sleep mode. When λ_f/λ_o increases, P_i will be dominated by the power consumption of the WLAN receiver module. As λ_f/λ_o increases, it is more likely that the packets are delivered through WLAN with higher transmission rate, and smaller $E[t_w]$ values are observed. In these figures, $E[t_w]$ is a decreasing function of λ_f/λ_o.

Effects of the mean reading time $1/\lambda_{pc}$. Figure 5 shows the effects of $1/\lambda_{pc}$ on P_i and $E[t_w]$. Figure 5 (a) shows that when $\lambda_f/\lambda_o > 10^0$, $1/\lambda_{pc}$ has minor impact on P_i. When λ_f/λ_o is larger, the MS has a higher probability to stay in a WLAN ON period. In this case, most of the packets are delivered through the WLAN connection, and the UMTS receiver is switched into the sleep mode. Compared with the WLAN power consumption in ON periods, the UMTS power consumption in sleep mode is relatively small and can be ignored. Therefore, changing the packet traffic pattern (via adjusting the reading time) does not have a significant influence on P_i.

On the other hand, when $\lambda_f/\lambda_o \leq 10^0$, P_i slightly increases when $10^0 E[t_x] \leq 1/\lambda_{pc} \leq 10^3 E[t_x]$, and then slightly decreases when $10^3 E[t_x] \leq 1/\lambda_{pc} \leq 10^5 E[t_x]$. When $\lambda_f/\lambda_o \leq 10^0$, longer WLAN OFF periods are observed, and the packet arrivals have larger chance to be forwarded to the RNC. Therefore, P_i performance depends on the behavior of the UMTS receiver. More specifically, P_i is determined by the ETSI traffic parameters and the power consumption parameters of the UMTS receiver module. Under the considered parameter settings in Figure 5 (a), when $1/\lambda_{pc} \rightarrow 10^0 E[t_x]$, P_i is dominated by the UMTS sleep mode operation, and the corresponding value is less than 0.4 watts. As $1/\lambda_{pc}$ increases, the MS experiences longer inactivity periods. Compared with sleep periods, inactivity periods (with power consumption 0.4 watts) are relatively power-consuming. Therefore, P_i increases accordingly. However, when $1/\lambda_{pc} > t_I$ (i.e., $1000E[t_x]$), increasing $1/\lambda_{pc}$ will not further increase the length of inactivity periods. In contrast, longer sleep periods with low power consumption will be observed. Thus, P_i decreases as $1/\lambda_{pc}$ increases.

As shown in Figure 5 (b), when λ_f/λ_o is smaller (e.g., $\lambda_f/\lambda_o < 10^1$), $E[t_w]$ decreases when $E[t_x] \leq 1/\lambda_{pc} \leq 10^2 E[t_x]$, and then increases when $10^3 E[t_x] < 1/\lambda_{pc} < 10^5 E[t_x]$.

The smaller λ_f/λ_o leads the MS to exercise the UMTS DRX mechanism to receive packets from the RNC. When $1/\lambda_{pc} < 10^2 E[t_x]$, packets arrive too fast to be served by the RNC, and most of the packets are queued in the RNC buffer. For this reason, the mean packet waiting time $E[t_w]$ increases as $1/\lambda_{pc}$ decreases. When $1/\lambda_{pc} \geq 10^3 E[t_x]$, the MS enters the power saving mode more frequently, and the $E[t_w]$ increases gradually as $1/\lambda_{pc}$ increases. We note that the above effect is less obvious in higher λ_f/λ_o cases (e.g., $\lambda_f/\lambda_o = 10^3$). This is because higher λ_f/λ_o ratio results in that packets are mainly served by the WLAN, and these packets can be delivered immediately.

Effects of the length of a DRX cycle t_D. Figure 6 (a) shows the intuitive result that P_i is a decreasing function of the length of a DRX cycle t_D. Power consumption in the power saving mode is influenced by τ/t_D. In this figure, we set τ as a fixed value. As t_D increases, the proportion of the listening period in a DRX cycle decreases, and therefore P_i decreases accordingly. We observe that when $t_D > 10^2 E[t_x]$, the listening period in a DRX cycle is always within 1%. Consequently, increasing t_D can not further improve the P_i performance.

Figure 6 (b) shows that $E[t_w]$ is an increasing function of t_D. When t_D is larger (e.g., $t_D > 10E[t_x]$), the probability that a packet arrives during a sleep period is higher. The $E[t_w]$ significantly increases as t_D increases. With a small t_D value (e.g., $t_D < 10E[t_x]$), the MS is most likely to be in a listening period even if the packet arrives during a DRX cycle (i.e., the MS wakes up to listen to the paging channel), and $E[t_w]$ is dominated by the waiting time in the RNC buffer. In this case, decreasing t_D rarely improves the $E[t_w]$ performance. From the above observations, we suggest that t_D should be selected in the range $[10E[t_x], 100E[t_x]]$.

Effects of the threshold t_I of the RNC inactivity timer. With smaller t_I, the UMTS receiver module enters the sleep mode soon after each busy period, which lowers P_i and increases $E[t_w]$. Figure 7 (a) shows a general phenomenon that P_i remains stable when t_I is smaller than a small threshold ϵ_s, then increases rapidly when $\epsilon_s < t_I < \epsilon_l$ (where ϵ_l is another threshold larger than ϵ_s), and then turns to be stable when $t_I > \epsilon_l$. For example, for the "$*$" curve (i.e., $\lambda_f/\lambda_o = 10^{-3}$), $\epsilon_s \simeq 10^2 E[t_x]$ and $\epsilon_l \simeq 10^5 E[t_x]$. When $t_I < \epsilon_s$, packets are not likely to arrive before the RNC timer expires, and the MS can enter the sleep mode to reduce the power consumption. With increasing of

t_I, this effect becomes minor, and we observe that P_i increases rapidly. When $t_I > \epsilon_l$, the MS almost always stays in busy or inactivity periods. Hence, no power saving is possible, and stable and larger P_i values are observed. We also note that the values of ϵ_s and ϵ_l depend on the setting of λ_f/λ_o. As λ_f/λ_o increases, ϵ_s and ϵ_l increase.

As shown in Figure 7 (b), for $E[t_w]$, we observe the opposite phenomenon. That is, $E[t_w]$ remains stable when t_I is smaller than a small threshold ϵ_s, then decreases rapidly when $\epsilon_s < t_I < \epsilon_l$ (where ϵ_l is another threshold larger than ϵ_s), and then turns to be stable when $t_I > \epsilon_l$. The reason is given as follows. A larger t_I value implies a higher probability that the MS stays in an inactivity period when packets arrive. In this case, the packets have better chance to be served immediately, and lower $E[t_w]$ is expected.

5 Conclusions

This paper proposed an analytical model and conducted simulation experiments to investigate the power consumption of a dual-mode MS in terms of the *power consumption indicator* P_i and the *mean packet waiting time* $E[t_w]$. Our study indicated the following. The λ_f/λ_o ratio has conflicting impacts on $P_{i,w}$ and $P_{i,u}$. More specifically, as λ_f/λ_o increases, $P_{i,w}$ increases while $P_{i,u}$ decreases. We observed reverse effects of λ_f/λ_o on $E[t_w]$, and $E[t_w]$ becomes more sensitive for a smaller λ_f/λ_o than a larger λ_f/λ_o. Under the parameter settings recommended in the ETSI traffic model, P_i increases and then decreases as the mean reading time increases, and t_D should be chosen from the range $[10E[t_x], 100E[t_x]]$. We also found that in some t_I settings, a higher λ_f/λ_o consumes less power than a lower λ_f/λ_o. We gave an interpretation for this phenomenon.

A Simulation Model

This section describes the discrete event-driven simulation model that simulates the power consumption behavior of an MS in the GAN and UMTS interworking environment. We define six types of events listed as follows:

- The ARRIVAL event represents a packet arrival to the SGSN.

- The DEPARTURE event implies that a packet has been successfully transmitted to the MS.
- The WLAN_ON event represents that WLAN connectivity enters an ON period from an OFF period, i.e., the WLAN connection becomes available.
- The WLAN_OFF event represents that WLAN connectivity enters an OFF period from an ON period, i.e., the WLAN connection becomes unavailable.
- The SLEEP event represents that an inactivity period of the MS ends, and the MS enters a sleep period.
- The WAKEUP event represents that the MS wakes up from a sleep period.

A timestamp is maintained in each event to indicate when the event occurs. Events are inserted into an event list and are deleted/processed from the list in a non-decreasing timestamp order. During the execution of simulation, a simulation clock t_s is maintained to indicate the progress of the simulation. The following variables are used in the simulation model:

- t_a stores the inter-packet arrival time.
- t_x stores the packet service time.
- t_o stores the length of a WLAN ON period.
- t_f stores the length of a WLAN OFF period.

The following counters are used in our simulation model to calculate the output measures (to be elaborated on later):

- N_a counts the total number of ARRIVAL events.
- N_w counts the total number of WAKEUP events.
- T_b calculates the total time when the MS is in the UMTS busy periods.
- T_i calculates the total time when the MS is in the UMTS inactivity periods.

- T_s calculates the total time when the MS is in the UMTS sleep periods.
- T_o calculates the total time when the MS is in the WLAN ON periods.
- T_f calculates the total time when the MS is in the WLAN OFF periods.
- T_w calculates the total waiting time for queued packets.

We repeat the simulation runs until N_a exceeds the constant MAXARRIVAL, which is a fixed and sufficiently large positive number, to ensure the stability of the simulation results. Two output measures are investigated in our model, including the power consumption indicator P_i and the mean packet waiting time $E[t_w]$, which are obtained as follows:

$$P_i = \frac{T_b P_{u,b} + T_i P_{u,i} + (T_s - N_w \tau) P_{u,s} + N_w \tau P_{u,l} + T_o P_{w,o} + T_f P_{w,f}}{t_s} \quad (23)$$

and

$$E[t_w] = \frac{T_w}{N_a}, \quad (24)$$

where $P_{u,b}$, $P_{u,i}$, $P_{u,s}$, $P_{u,l}$, $P_{w,o}$, $P_{w,f}$ and τ are defined in Section 3.

Figure 8 illustrates the flowchart of our simulation model. The variable `UmtsState` stores the state of the MS's UMTS receiver, whose value can be busy, inactivity or sleep. The variable `WlanState` stores the state of the MS's WLAN receiver, whose value can be on or off. The two variables $t_{p,u}$ and $t_{p,w}$ store the times when the last changes of `UmtsState` and `WlanState` occur, respectively. We maintain a FIFO list denoted as RNC_buffer to buffer the ARRIVAL events that can not be served immediately. The execution of the simulation model is described as follows.

Step 1 sets up the input parameters (including λ_o, λ_f, t_I, t_D, etc.). In addition, the counters (e.g., N_a, N_w, T_b, T_s, T_f, t_s, and $t_{p,w}$) are set to zero, and the event list is set to NULL. Step 2 sets `UmtsState` to inactivity. Step 3 generates a WLAN_ON event and an ARRIVAL event. The timestamp of the WLAN_ON event is set to 0. We generate a t_a value following the exponential distribution with rate λ_a or following the ETSI traffic model. The timestamp of the ARRIVAL event is set to t_a. The WLAN_ON and ARRIVAL events are inserted into the event list. Step 4 removes the next event e from the event list, and set the value of t_s to e.timestamp. Step 5 checks the type of event e.

If event e is an ARRIVAL event at Step 5, Step 6 checks whether N_a is equal to MAXARRIVAL. If so, Step 7 computes the output measures using (23) and (24), and the simulation terminates. Otherwise (i.e., $N_a <$ MAXARRIVAL), Step 8 increases N_a by one. Step 9 generates the next ARRIVAL event, whose timestamp is set to $t_s + t_a$ (where t_a is randomly generated following the exponential distribution with rate λ_a or is generated following the ETSI traffic model). Then this new ARRIVAL event is inserted into the event list. Step 10 checks whether `WlanState` is equal to on. If so, the simulation goes back to Step 4. This is because the WLAN connection supports high data transmission rate, and we assume that the service time and waiting time of the ARRIVAL event e in GAN can be ignored. On the other hand, if `WlanState` is equal to off, Step 11 checks whether `UmtsState` is equal to inactivity. If so (i.e., the MS is in an inactivity period), due to the packet arrival, the MS enters a new busy period. Step 12 removes the SLEEP event (corresponding to this inactivity period) from the event list. Step 13 sets `UmtsState` to busy. Step 14 sets $T_i \leftarrow T_i + t_s - t_{p,u}$ and $t_{p,u} \leftarrow t_s$. Step 15 generates a DEPARTURE event (corresponding to this ARRIVAL event) with timestamp $t_s + t_x$ (where t_x is randomly generated following the general distribution with mean $1/\lambda_x$ and variance V_x or is generated following the ETSI traffic model), and then inserts it into the event list. If `UmtsState` $\neq$ inactivity at Step 11 (i.e., `UmtsState` = busy or sleep), the packet arrival can not be served. Step 16 inserts the ARRIVAL event into the RNC_buffer list.

If event e is a DEPARTURE event at Step 5, Step 17 checks whether there is any ARRIVAL event in the RNC_buffer list. If so, Steps 18-20 are executed to select a buffered packet arrival for transmission. Step 18 removes the first ARRIVAL event (denoted as e_b) from the RNC_buffer list. Step 19 sets $T_w \leftarrow T_w + t_s - e_b$.timestamp. Step 20 generates a DEPARTURE event (corresponding to the ARRIVAL event e_b) with timestamp $t_s + t_x$ (where t_x is randomly generated following the general distribution with mean $1/\lambda_x$ and variance V_x or is generated following the ETSI traffic model), and then inserts it into the event list. The simulation goes back to Step 4. If the RNC_buffer list is NULL at Step 17, Step 21 sets `UmtsState` to inactivity. At Step 22, T_b is set to $T_b + t_s - t_{p,u}$ and $t_{p,u}$ is set to t_s. Step 23 generates a SLEEP event with timestamp $t_s + t_I$, and then inserts it into the event list. The simulation returns to Step 4.

If event e is a SLEEP event at Step 5, `UmtsState` is set to sleep at Step 24. We update T_i and $t_{p,u}$ as $T_i \leftarrow T_i + t_s - t_{p,u}$ and $t_{p,u} \leftarrow t_s$ at Step 25. Step 26 generates a WAKEUP event with timestamp $t_s + t_D$, and then inserts it into the event list. The simulation goes back to Step 4.

If event e is a WAKEUP event at Step 5, Step 27 increases N_w by one. Step 28 checks whether the RNC_buffer list is NULL. If not (i.e., there are buffered packet arrivals), Step 29 removes the first ARRIVAL event e_b from the RNC_buffer list to process. Step 30 sets $T_w \leftarrow T_w + t_s - e_b$.timestamp. The `UmtsState` is set to busy at Step 31. Step 32 updates T_s and $t_{p,u}$ as $T_s \leftarrow T_s + t_s - t_{p,u}$ and $t_{p,u} \leftarrow t_s$. Step 33 generates a DEPARTURE event corresponding to the ARRIVAL event e_b with timestamp $t_s + t_x$ (where t_x is randomly generated following the general distribution with mean $1/\lambda_x$ and variance V_x or is generated following the ETSI traffic model), and then inserts it into the event list. If the RNC_buffer list is NULL at Step 28, Step 34 generates the next WAKEUP event with timestamp $t_s + t_D$, and then inserts it into the event list. The simulation returns to Step 4.

If event e is a WLAN_ON event at Step 5, Steps 35-37 are executed to activate a WLAN ON period. Step 35 sets `WlanState` to on. Step 36 updates T_f and $t_{p,w}$ as $T_f \leftarrow T_f + t_s - t_{p,w}$ and $t_{p,w} \leftarrow t_s$, respectively. Step 37 generates a WLAN_OFF event (corresponding to this WLAN ON period) with timestamp $t_s + t_o$ (where t_o is randomly generated following the exponential distribution with rate λ_o), and then inserts it into the event list. The simulation goes back to Step 4.

If event e is a WLAN_OFF event at Step 5, Step 38 sets `WlanState` to off. Step 39 updates T_o and $t_{p,w}$ as $T_o \leftarrow T_o + t_s - t_{p,w}$ and $t_{p,w} \leftarrow t_s$, respectively. Step 40 generates a WLAN_ON event (corresponding to this WLAN OFF period) with timestamp $t_s + t_f$ (where t_f is randomly generated following the exponential distribution with rate λ_f), and then inserts the generated event into the event list. The simulation returns to Step 4.

References

[1] 3rd Generation Partnership Project; Technical Specification Group GSM/EDGE Radio Access Network. Generic Access to the A/Gb Interface; Stage 2. Technical Specification 3GPP TS 43.318 version 6.6.0, 3GPP, April 2006.

[2] 3rd Generation Partnership Project; Technical Specification Group Radio Access Network. RRC Protocol Specification for Release 1999. Technical Specification 3GPP TS 25.331 version 3.5.0, 3GPP, December 2000.

[3] Bluetooth Special Interest Group. Bluetooth Core Specification v2.0. Technical Standard, Bluetooth SIG, November 2004.

[4] Chen, Z.-H. and Lin, J.-C. Technical Slides: WCDMA Current Power Consumption. Inventec Appliances Corp., December 2006.

[5] Daigle, J.N. *Queueing Theory for Telecommunications*. Addison-Wesley, 1992.

[6] Doufexi, A., Tameh, E., Nix, A., Armour, S., and Molina, A. Hotspot Wireless LANs to Enhance the Performance of 3G and Beyond Cellular Networks. *IEEE Communications Magazine*, 41(7):58–65, July 2003.

[7] European Telecommunications Standards Institute. Universal Mobile Telecommunications System (UMTS); Selection Procedures for the Choice of Radio Transmission Technologies of the UMTS. Technical Report TR 101 112 (UMTS 30.03) version 3.2.0, ETSI, April 1998.

[8] Hämäläinen, S., Holma, H., and Sipilä, K. Advanced WCDMA Radio Network Simulator. *Proc. of PIMRC*, pages 509–604, September 1999.

[9] IEEE. Wireless Medium Access Control (MAC) and Physical Layer (PHY) Specifications. Technical Standard IEEE Standard 802.11, IEEE, April 1997.

[10] Johnson, N.L. *Continuous Univariate Distributions*, volume 1. John Wiley& Sons, 1970.

[11] Law, A.M. and Kelton, W.D. *Simulation Modeling and Analysis*. McGraw-Hill Higher Education, 3rd edition, 2000.

[12] Lee, C.-C., Yeh, J.-H., and Chen J.-C. Impact of Inactivity Timer on Energy Consumption in WCDMA and cdma2000. *Wireless Telecommunications Symposium*, May 2004.

[13] Lin, P., Lin, Y.-B., and Chlamtac, I. Modeling Frame Synchronization for UMTS High-Speed Downlink Packet Access. *IEEE Transactions on Vehicular Technology*, 52(1):132–141, January 2003.

[14] Lin, Y.-B. and Chuang, Y.-M. Modeling the Sleep Mode for Cellular Digital Packet Data. *IEEE Communications Letters*, 3(3):63–65, March 1999.

[15] Nguyen, H.N. and Sasase, I. Downlink Queuing Model and Packet Scheduling for Providing Lossless Handoff and QoS in 4G Mobile Networks. *IEEE Transactions on Mobile Computing*, 5(5):452–462, May 2006.

[16] Ross, S.M. *Stochastic Processes*. John Wiley, New York, 2nd edition, 1996.

[17] Shih, E., Bahl, P., and Sinclair, M.J. Wake on Wireless: An Event Driven Energy Saving Strategy for Battery Operated Devices. *Proc. of MobiCom*, September 2002.

[18] UMA Consortium. Unlicensed Mobile Access (UMA) Architecture (Stage 2). R1.0.0, Technical Specification, September 2004.

[19] Yang, S.-R. and Lin, Y.-B. Modeling UMTS Discontinuous Reception Mechanism. *IEEE Transactions on Wireless Communications*, 4(1):312–319, January 2005.

[20] Zheng, R., Hou, J.C. and Sha, L. Performance Analysis of Power Management Policies in Wireless Networks. *IEEE Transactions on Wireless Communications*, 5(6):1351–1361, June 2006.

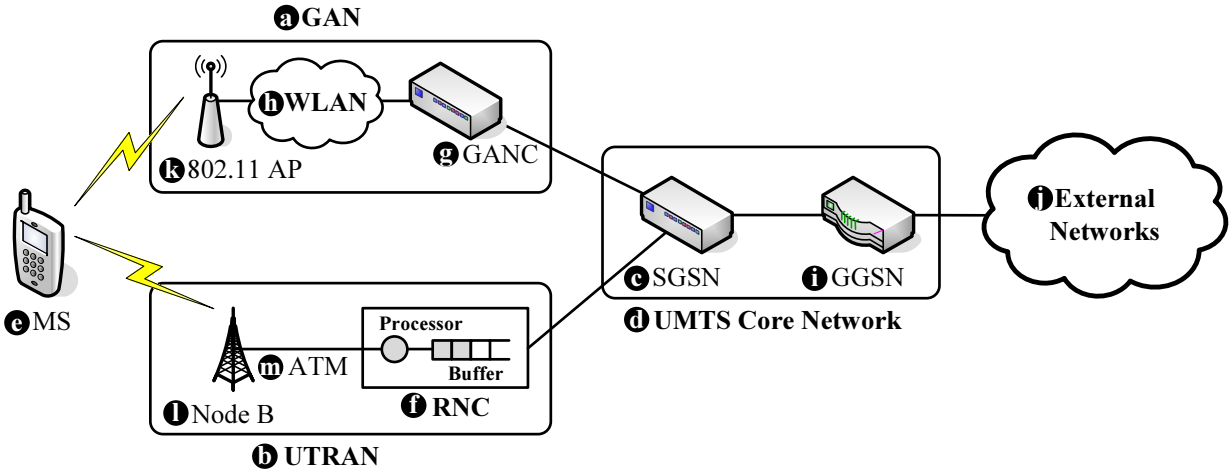

GAN: Generic Access Network
GANC: Generic Access Network Controller
AP: Access Point
MS: Mobile Station
UTRAN: UMTS Terrestrial Radio Access Network
RNC: Radio Network Controller
Node B: Base Station
GGSN: Gateway GPRS Support Node
SGSN: Serving GPRS Support Node

Figure 1: The system model for the GAN and UMTS interworking

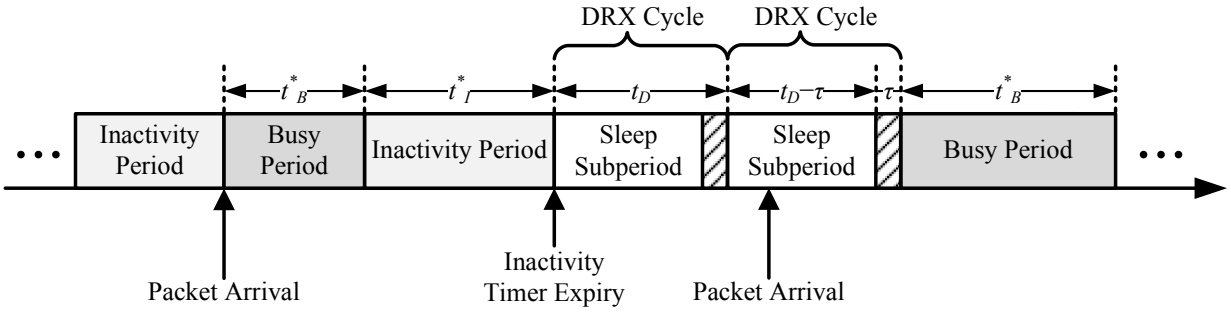

Figure 2: UMTS Discontinuous Reception (DRX) mechanism

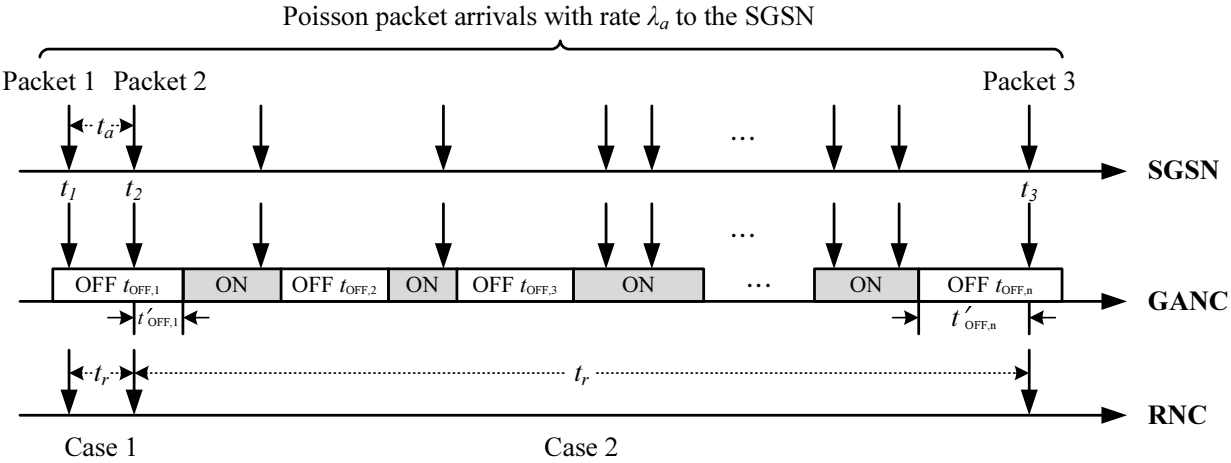

Figure 3: Timing diagram

Table 1: Comparison between the analysis and simulation results ($V_x = 1/\lambda_x^2$, $t_I = 60/\lambda_x$, $t_D = 10/\lambda_x$, $\tau = 0.1/\lambda_x$, and $\lambda_a = 0.1\lambda_x$)

Power consumption indicator ($\lambda_o = 10\lambda_x$)					
λ_f	$10^{-2}\lambda_o$	$10^{-1}\lambda_o$	$10^{0}\lambda_o$	$10^{1}\lambda_o$	$10^{2}\lambda_o$
P_i (Analytical)	0.545077	0.581327	0.747810	0.729542	0.627239
P_i (Simulation)	0.545242	0.581309	0.747863	0.729607	0.627323
Error	0.03034%	0.00302%	0.00718%	0.00886%	0.01335%

Mean packet waiting time ($\lambda_o = 10\lambda_x$)					
λ_f	$10^{-2}\lambda_o$	$10^{-1}\lambda_o$	$10^{0}\lambda_o$	$10^{1}\lambda_o$	$10^{2}\lambda_o$
$E[t_w]$ (Analytical)	0.129287	0.120440	0.182379	0.269256	0.046673
$E[t_w]$ (Simulation)	0.129425	0.120748	0.182674	0.269372	0.046861
Error	0.10719%	0.25549%	0.16206%	0.04283%	0.40427%

Approximation for Theorem 1 ($\lambda_f = 10^{0}\lambda_o$)					
λ_o	$10^{-5}\lambda_x$	$10^{-3}\lambda_x$	$10^{-1}\lambda_x$	$10^{0}\lambda_x$	$10^{1}\lambda_x$
P_i (Analytical)	0.747810	0.747810	0.747810	0.747810	0.747810
P_i (Simulation)	0.574693	0.581841	0.728581	0.746172	0.747612
Error	23.1499%	22.1940%	2.57138%	0.21904%	0.02648%
$E[t_w]$ (Analytical)	0.182379	0.182379	0.182379	0.182379	0.182379
$E[t_w]$ (Simulation)	0.066068	0.099804	0.303903	0.202309	0.185555
Error	63.7743%	45.2766%	66.6327%	10.9278%	1.74143%

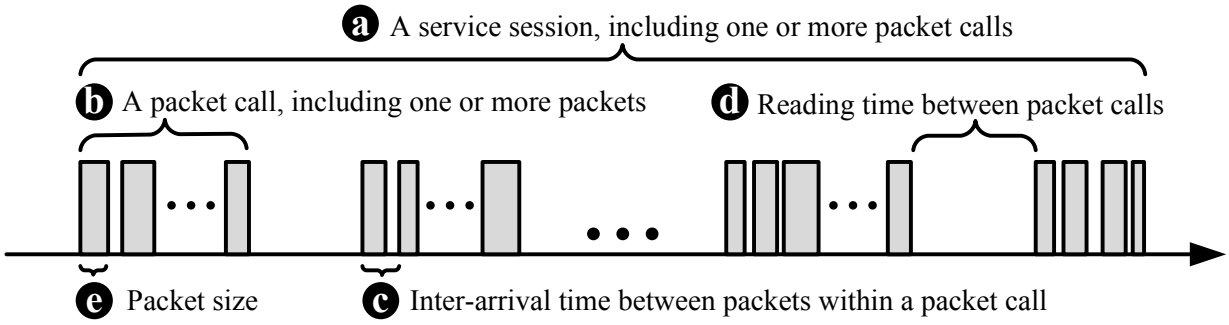

Figure 4: The characteristic of a service session

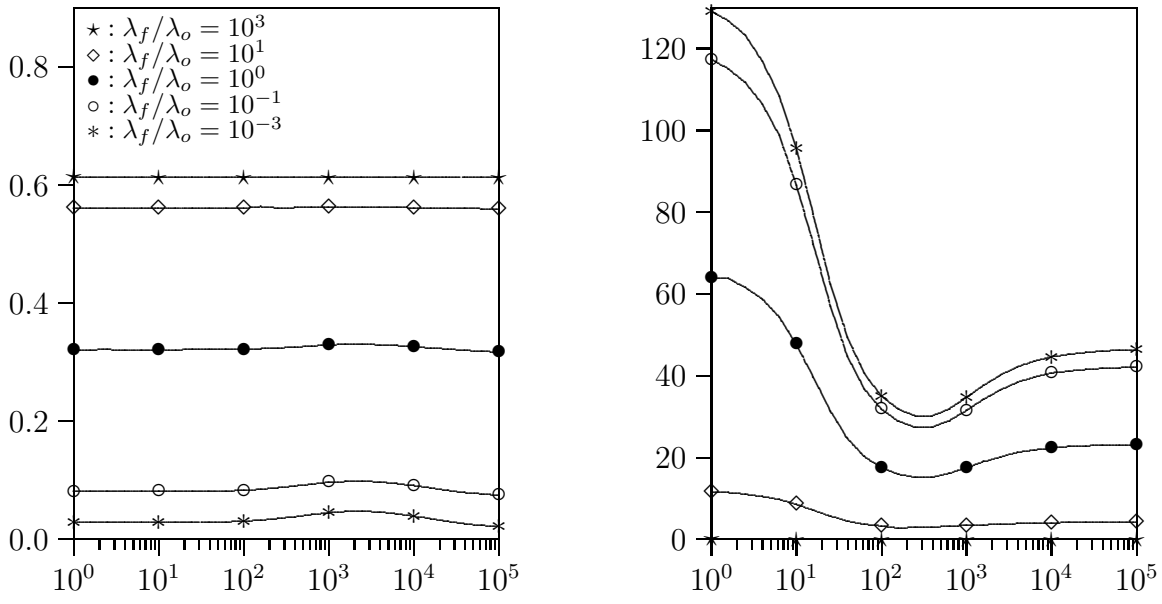

(a) P_i (unit: watt) (b) $E[t_w]$ (unit: $E[t_x]$)

Figure 5: Effects of $1/\lambda_{pc}$ and λ_f/λ_o ($\lambda_o = \lambda_x/20000$, $t_D = 50E[t_x]$, $t_I = 1000E[t_x]$, $\tau = E[t_x]$, $\lambda_{is} = \lambda_x/50000$, $\lambda_p = 10\lambda_x$, $\mu_{pc} = 5$, and $\mu_p = 25$)

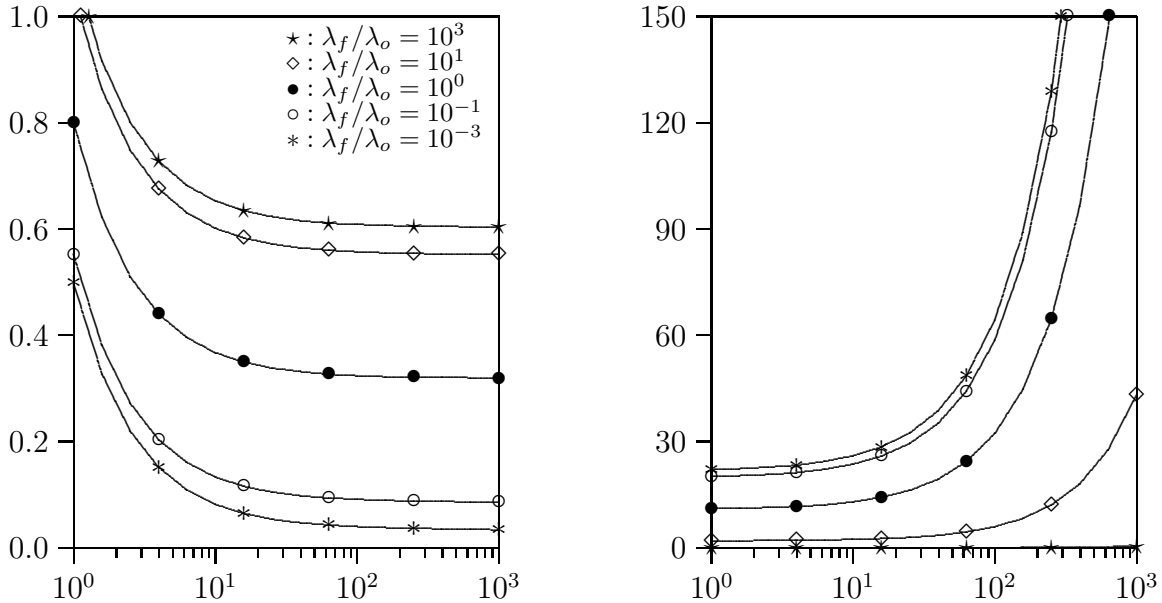

(a) P_i (unit: watt) (b) $E[t_w]$ (unit: $E[t_x]$)

Figure 6: Effects of t_D and λ_f/λ_o ($\lambda_o = \lambda_x/20000$, $t_I = 1000E[t_x]$, $\tau = E[t_x]$, $\lambda_{is} = \lambda_x/50000$, $\lambda_{pc} = \lambda_x/5000$, $\lambda_p = 10\lambda_x$, $\mu_{pc} = 5$, and $\mu_p = 25$)

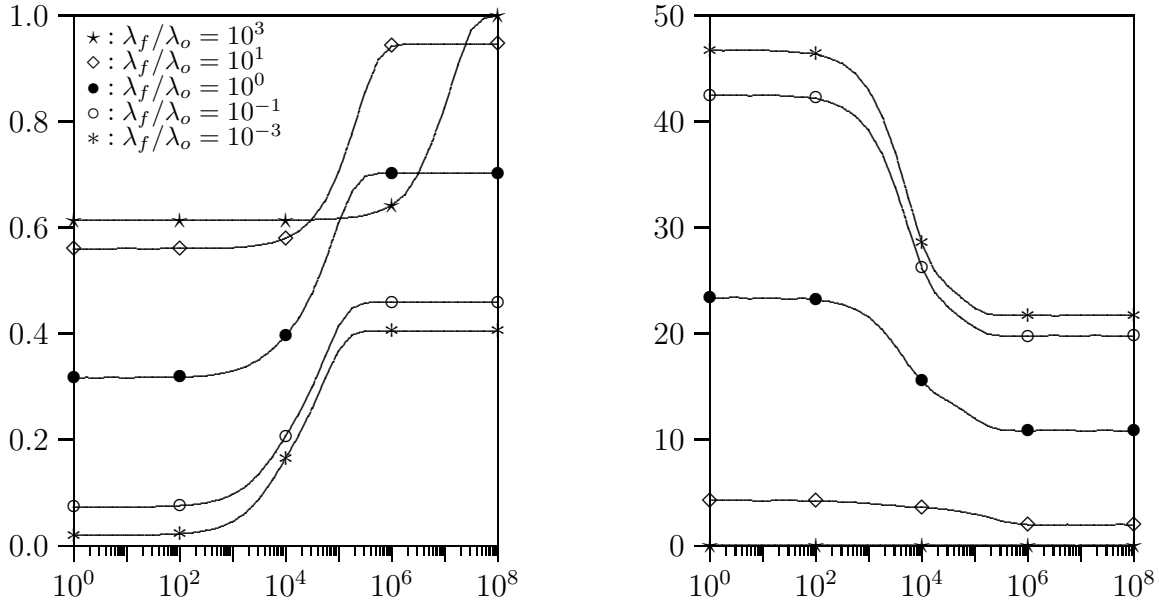

(a) P_i (unit: watt) (b) $E[t_w]$ (unit: $E[t_x]$)

Figure 7: Effects of t_I and λ_f/λ_o ($\lambda_o = \lambda_x/20000$, $t_D = 50E[t_x]$, $\tau = E[t_x]$, $\lambda_{is} = \lambda_x/50000$, $\lambda_{pc} = \lambda_x/5000$, $\lambda_p = 10\lambda_x$, $\mu_{pc} = 5$, and $\mu_p = 25$)

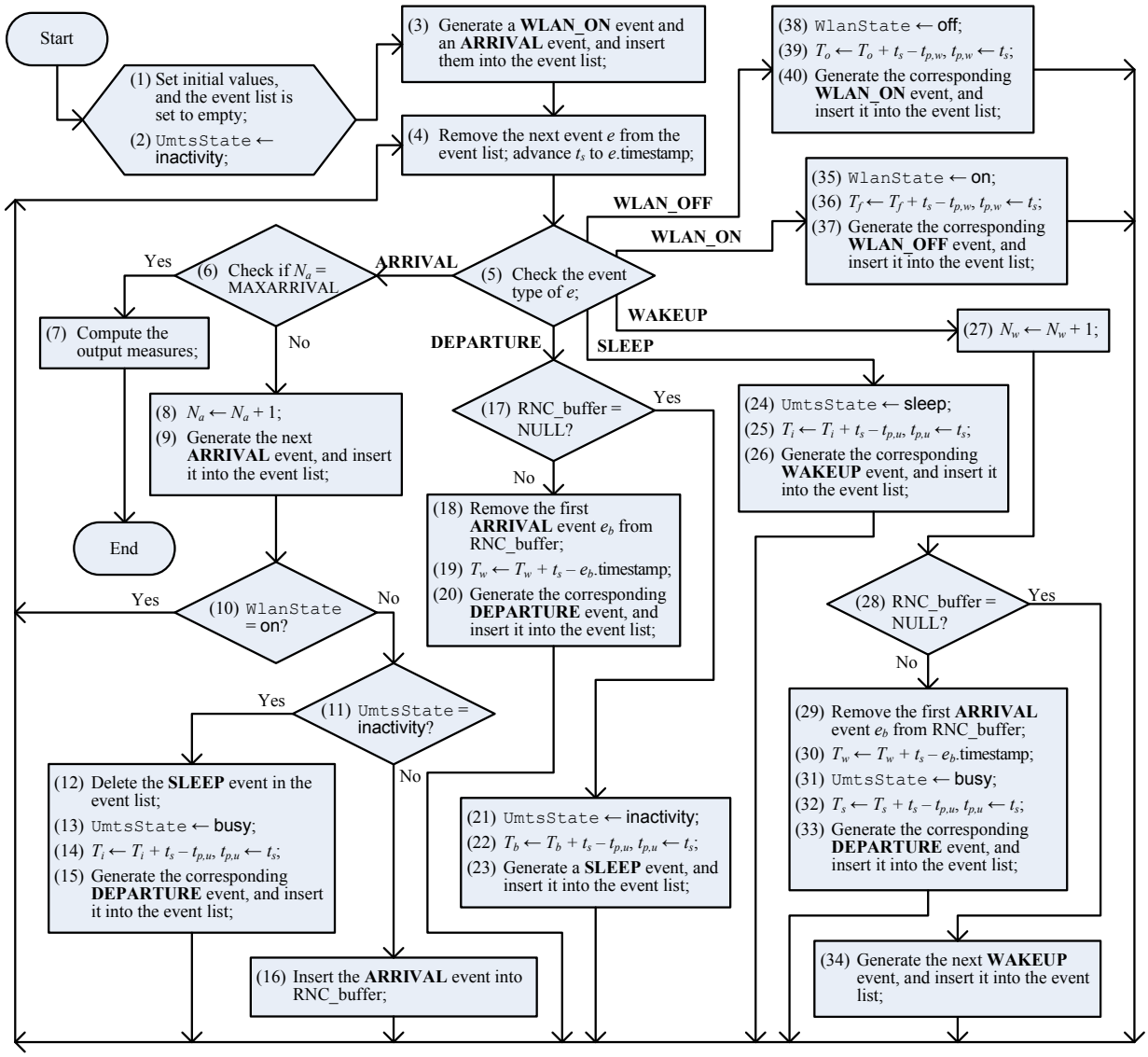

Figure 8: Flowchart of the simulation model